The effect of water table fluctuation on soil respiration in a lower coastal plain forested wetland in the southeastern U.S.

Guofang Miao,[1] Asko Noormets,[1] Jean-Christophe Domec,[1,2] Carl C. Trettin,[3] Steve G. McNulty,[4] Ge Sun,[4] and John S. King[1]

[1] Anthropogenic and environmental pressures on wetland hydrology may trigger changes in carbon (C) cycling, potentially exposing vast amounts of soil C to rapid decomposition. We measured soil CO_2 efflux (R_s) continuously from 2009 to 2010 in a lower coastal plain forested wetland in North Carolina, U.S., to characterize its main environmental drivers. To understand and quantify the spatial variation due to microtopography and associated differences in hydrology, measurements were conducted at three microsites along a microtopographic gradient. The seasonal hysteresis in R_s differed by microtopographic location and was caused by the transitions between flooded and nonflooded conditions. Because flooded R_s was small, we reported R_s dynamics mainly during nonflooded periods. A nested model, modified from conventional Q_{10} (temperature sensitivity) model with dynamic parameters, provided a significantly better simulation on the observed variation of R_s. The model performed better with daily data, indicating that soil temperature (T_s) and water table depth (WTD) were the primary drivers for seasonal variation. The diel variation of R_s was high and independent of T_s and WTD, which both had small diel variations, suggesting the likely association with plant activity. Overall, the site-average soil CO_2 efflux was approximately 960–1103 $g\,C\,m^{-2}\,yr^{-1}$ in 2010, of which 93% was released during nonflooded periods. Our study indicates that R_s is highly linked to hydroperiod and microtopography in forested wetlands and droughts in wetlands will accelerate soil C loss.

1. Introduction

[2] It is estimated that wetland soils store 18–30% of the 1550 Pg of total global soil carbon while covering only 2–3% of the land area [*Trettin and Jurgensen*, 2003]. Information on soil carbon dynamics in wetlands, however, is very limited despite the large amount of C stored in these ecosystems. For example, in the global soil respiration database (SRDB version 20100517) [*Bond-Lamberty and Thomson*, 2010], there are only 135 data records for wetlands among the total of 3821 records. From this database, the global average annual soil CO_2 efflux (R_s, also representing the term of "soil respiration" in this study) from wetlands was 344 ± 278 (mean ± SD) $g\,C\,m^{-2}\,yr^{-1}$ as compared to an average $816 \pm 516\,g\,C\,m^{-2}\,yr^{-1}$ in upland ecosystems. Yet, while the reported effluxes from wetlands have been smaller than from upland systems, models suggest that wetland soil decomposition may be more sensitive to changing climate [*Ise et al.*, 2008] and thus represent an important positive feedback loop.

[3] Simulating soil carbon dynamics in wetlands has proven more challenging than in upland ecosystems due to the two physical characteristics, hydrologic regime and microtopography [*Barry et al.*, 1996; *Mitsch and Gosselink*, 2007]. The seasonal variation of hydrologic regime, i.e., hydroperiod, can confound understanding of temporal variation on R_s in addition to the general seasonal variation regulated by temperature [*Mitsch and Gosselink*, 2007]. The dynamic boundary of water table induces changes between aerobic and anaerobic status and also influences R_s through soil water content (SWC) or substrate availability to biological processes [*Wheeler*, 1999]. Microtopography, interacting with hydrologic regime, is associated with plant distributions and soil chemical and physical properties [*Ehrenfeld*, 1995; *Frei et al.*, 2012; *Jones et al.*, 1996; *Van der Ploeg et al.*, 2012; *Waddington and Roulet*, 1996]. However, only a few studies included the microtopography factor into the design of field experiments, which could significantly affect the estimate of

---

R_s at the ecosystem scale and the role of wetlands in the global carbon cycle [*Alm et al.*, 1997, 1999; *Jauhiainen et al.*, 2005; *Luken and Billings*, 1985].

[4] The mechanistic response of R_s to its main environmental drivers remains poorly characterized for wetlands [*Davidson et al.*, 2006; *Lloyd and Taylor*, 1994; *Luo and Zhou*, 2006]. Generally, in wetlands the response of R_s to temperature is similar to upland ecosystems, especially under aerobic conditions (e.g., most wetland studies in SRDB). The effects of soil water content, however, usually result in different patterns of R_s between wetlands and upland ecosystems. During dry seasons or drought events, the aerobic R_s increases in wetlands when the water table drops below the surface and oxygen and substrate availabilities increase correspondingly [*Laiho*, 2006; *Mast et al.*, 1998; *Schreader et al.*, 1998]. In upland ecosystems dry conditions represent a significant decrease in soil water content and R_s decreases [*Law et al.*, 2001; *Reichstein et al.*, 2002; *Wen et al.*, 2010]. Integrating effects of both temperature and soil water content imply that in wetlands the warmer and drier conditions may stimulate R_s whereas in many upland ecosystems drier conditions likely offset the increase in R_s that would result from warming. Therefore, similarity in temperature effects implies the possibility of applying the R_s models for upland ecosystems into wetlands, but accounting for variation in SWC or water table depth (WTD) requires a different model structure.

[5] Most previous studies suggested that WTD is a better indicator than SWC for investigating R_s in wetlands (studies included in SRDB; *Bond-Lamberty and Thomson* [2010]), and many laboratory controlled studies have demonstrated the WTD effect qualitatively [*Blodau et al.*, 2004; *Dinsmore et al.*, 2009; *Moore and Dalva*, 1993; *Vicca et al.*, 2009]. However, adaptation of models across sites has been complicated by the confounding effects of temperature, large spatial variability, and methodological differences among studies [*Chimner*, 2004; *Kim and Verma*, 1992; *Mäkiranta et al.*, 2009; *Silvola et al.*, 1996]. It has been shown that without proper accounting of hydrologic effects or other confounding influences, using the short-term temperature sensitivity to project soil responses to global change could result in significant bias [*Falloon et al.*, 2011; *Subke and Bahn*, 2010].

[6] Efforts to quantify the effect of SWC or WTD on R_s (as well as on ecosystem respiration) have included SWC- or WTD-sensitive temperature sensitivity (e.g., Q_{10} in Q_{10} model or activation energy in Arrhenius equation) [*Mäkiranta et al.*, 2009; *Reichstein et al.*, 2002] as well as SWC-sensitive basal respiration (R_b) [*Gaumont-Guay et al.*, 2006; *Noormets et al.*, 2008]. While the dynamic characteristics of Q_{10} and R_b have been well recognized, its application and associated mechanisms are still a matter of debate due to the statistical interdependence of the parameters and confounding effects from other factors [*Janssens and Pilegaard*, 2003; *Kirschbaum*, 2006; *Mahecha et al.*, 2010; *Subke and Bahn*, 2010]. As the majority of studies have been conducted in upland forests, the dynamic characteristics of Q_{10} and R_b in wetlands are uncertain [*Davidson*, 2010; *Mahecha et al.*, 2010].

[7] Due to differences in topography and climate, wetlands develop different hydrology from uplands in the southeastern U.S. [*Sun et al.*, 2002] and consequently different biogeochemical cycling patterns. In the current study, we measured soil CO_2 efflux continuously from 2009 to 2010 in a seasonally flooded coastal forested wetland of North Carolina, U.S. The main objectives were the following: to (1) monitor the seasonal and spatial variations of R_s given the microtopographic heterogeneity, (2) characterize the main environmental drivers behind the observed variations of R_s, (3) develop a model for wetland R_s under aerobic conditions to account for the covarying effects of WTD and T_s, and (4) quantify the total soil CO_2 efflux by characterizing aerobic and anaerobic fluxes associated with the change in hydrologic regime.

2. Materials and Methods

2.1. Site Description

[8] The study site was located at the Alligator River National Wildlife Refuge on the Albemarle-Pamlico peninsula of North Carolina, U.S. (35°47′N, 75°54′W). This peninsula differs from coastlines to the north and the south because of the specific combination of geomorphic features and lagoonal environment, which results in astronomic tides being absent and rainfall being the main source of water [*Moorhead and Brinson*, 1995]. The peninsula has a deeper organic layer than the adjacent mainland areas due to having formed at the outlet of the Alligator River which carries organic sediments and for lower intensity of drainage due to very low topographic relief.

[9] Climate records from an adjacent meteorological station (Manteo AP, NC) show that the mean (1971–2000) annual precipitation is 1298 mm. Average annual temperature is 16.8°C with 6.8°C in January and 26.5°C in July. The overstory is predominantly composed of black gum (*Nyssa sylvatica*), swamp tupelo (*Nyssa biflora*), and bald cypress (*Taxodium distichum*), with occasional red maple (*Acer rubrum*), white cedar (*Chamaecyparis thyoides*), and loblolly pine (*Pinus taeda*). The understory is predominantly fetterbush (*Lyonia lucida*), bitter gallberry (*Ilex galbra*), and red bay (*Persea borbonia*). Canopy height ranges from 15 to 20 m, with peak leaf area index of 3.5 ± 0.3. Tree stand density was 2320 ± 800 stems ha^{-1} (~4 m^2/stem), and aboveground live biomass was estimated allometrically at 37.5 ± 12.5 Mg C ha^{-1} in 2009 and 2010. Average live fine-root biomass to a depth of 30 cm was 3.1 ± 1.0 Mg C ha^{-2} during the same period.

[10] Soils at this site are acidic with pH of 4.2–4.8 at surface horizons. Major soil types are poorly drained Pungo and Belhaven mucks. The amounts of organic matter in surface soils are approximately 40–100% and 20–100%, respectively. Moist bulk density of top organic soil is 0.35–0.60 and 0.40–0.65 g cm^{-3}, respectively (Web Soil Survey accessed on 14 December 2009). Dry bulk density from a soil survey when the site was flooded was approximately 0.06–0.10 g cm^{-3}. Due to the high porosity and as a result high permeability, the capillary effect is minimal at the top soils.

2.2. Micrometeorology and Water Table Measurement

[11] Precipitation was measured with a model TE-525 tipping bucket rain gauge (Texas Electronic, TX, U.S.), air temperature and humidity with a model HMP45AC (Vaisala, Helsinki, Finland), soil temperature (T_s) at 5 and 20 cm with a model CS107 gauge (Campbell Scientific (CSI), UT, U.S.) and WTD with a pressure water level data logger (Infinities, Port Orange, FL, U.S.). Volumetric SWC (CS 616, CSI) was also measured as a reference variable to WTD.
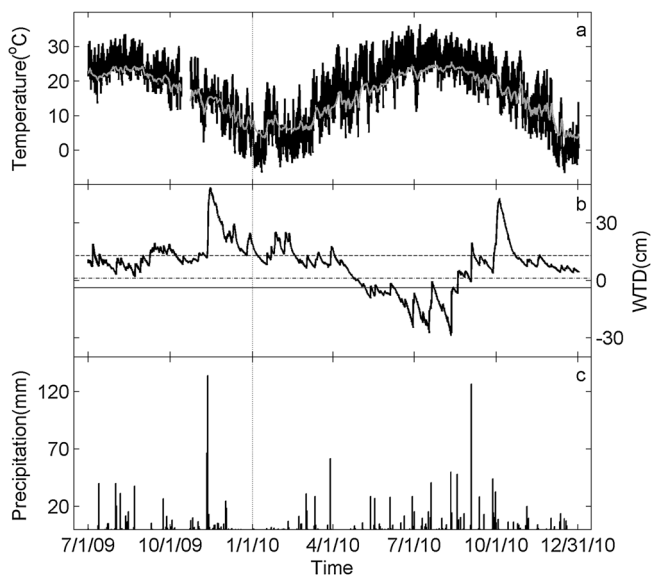
Figure 1. Seasonal variations observed in a lower coastal plain forested wetland in North Carolina, U.S., during 1 July 2009 to 31 December 2010 in (a) air temperature (grey line) and soil temperature at 5 cm depth (black line, T_s), (b) water table depth (WTD) at three microsites of varying elevation (HIGH: dashed line; MID: dash dot line; LOW: solid line), and (c) precipitation.

[12] During the 1.5 year observation period, 2009 was a relatively wet year and 2010 was a dry year. Water table depth during summer was significantly different between the two years. The monthly mean WTD was 9 and 8 cm for July and August, respectively, at the water table probe location, in 2009. The respective mean WTD was −14 and −7 cm (positive means water surface is above the ground and negative means below) for July and August in 2010. During autumn (September, October, and November), the mean WTD was 13 and 9 cm in 2009 and 2010, respectively. The seasonal variation of soil temperature was not significantly different between 2009 and 2010 (Figure 1).

2.3. Automated Soil CO₂ Efflux Measurement

[13] Soil CO_2 efflux was measured with an automated soil respiration measuring system consisting of a portable infrared gas analyzer (LI-8100, Licor Inc., NE, U.S.), multiplexer (LI-8150, Licor Inc.), and three permanent sampling chambers (8100–104, Licor Inc.). Three microsites were selected along a microtopography gradient. Microsite HIGH was at the base of a tree, microsite LOW was in the middle of a 2 m diameter nonvegetated low-lying area, and microsite MID was intermediate along the elevation gradient, and about half a meter away from the nearest tree. The HIGH microsite was elevated above water table for most of the year, whereas the MID and LOW were inundated for part of the year. The relative elevations of the three microsites of automatic measurements were 12.9, 1.2, and −3.8 cm relative to the elevation of water table probe location (Figure 1b). A 10 cm high PVC collar was installed at the HIGH microsite, and 25 cm high PVC collars were used at the MID and LOW microsite to allow the water table to fluctuate above the soil surface up to 20 cm. Four additional 2 foot long legs were attached onto each permanent

chamber in order to place them onto the tall collars and stand firmly in the water (see supporting information).

[14] Soil CO_2 efflux data were collected every 30 min from July 2009 to December 2010 with the automated system. On 11 November 2009, hurricane Ida resulted in 40 cm increase in the water table in 2 days, flooding the chambers and causing a 4 month data gap, as the system had to be repaired (dark grey areas in Figure 2). Measurements continued on 17 March 2010 and were discontinued again on 17 September due to hurricane Igor until 14 November. Data gaps were also caused by system protection under high relative humidity inside the chambers, occasional power problems at night, and excessive flux coefficient of variation. Data coverage was 28% of the time in 2009 and increased to above 50% as the result of improved power system management and less frequent high-humidity shutdown due to dry spring and summer of 2010. The LOW chamber was used for other purposes after 5 August 2010.

[15] Data were separated for the following modeling study to nonflooded and flooded subsets in terms of the WTD at each microsite, which corresponded to aerobic and anaerobic states, respectively. During the 1.5 year study, HIGH microsite had 90% of nonflooded records spanning all seasons in both 2009 and 2010. MID and LOW were not flooded only in spring and summer of 2010, with the percentages of 46% and 54% of the time, respectively. For the flooded records, due to the continuous change of surface water depth resulting in the change of collar headspace, the volume of headspace at each microsite was calculated based on the level of WTD above ground and the CO_2 effluxes were adjusted accordingly.

2.4. Survey Soil CO₂ Efflux Measurements

[16] Survey R_s measurements were conducted monthly in 2010 to supplement the automated measurements and characterize spatial variation. The survey system consisted of
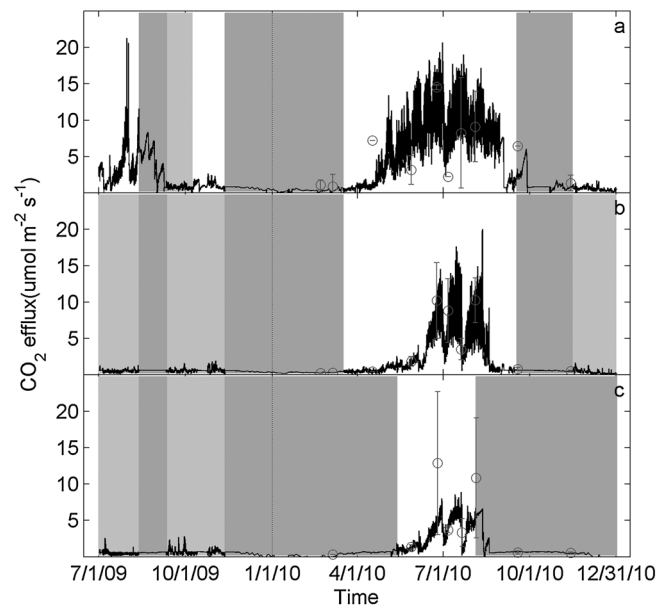

Figure 2. Soil CO_2 efflux at (a) HIGH, (b) MID, and (c) LOW microsites, respectively (nonflooded records: clear area; flooded records: light grey area; no measurements: dark grey area, filled with model results). Black solid line represents measurements by automated system, and grey circles with error bar (mean ± SD) represent survey measurements.
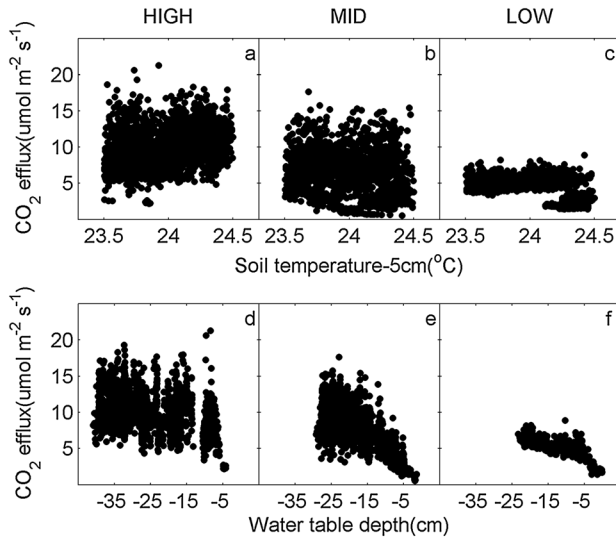
Figure 3. Relationship (a–c) between basal respiration (R_b) and soil temperature at 5 cm depth and (d–f) between R_b and water table depth at HIGH (in Figures 3a and 3d), MID (in Figures 3b and 3e), and LOW (in Figures 3c and 3f) microsites. R_b in this study was defined as respiration rate at 24°C. Soil CO_2 efflux data during nonflooded periods with the range of temperatures constrained to within ±0.5°C, i.e., 23.5–24.5°C, were separated out as R_b data.

LI-8100 and a portable survey chamber (LI 8100–103, Licor Inc.). Five 7 m diameter survey plots were installed in a 25 ha square area centered on the micrometeorology station, with one plot in the center and four plots at the four corners of the square. Six microsites were randomly selected within each plot and installed with 20 cm diameter PVC collars.

[17] The microtopography of each microsite was measured with a tripod-mounted laser level (RoboLaser Green RT-7210-1G, RoboToolz Inc., CA, U.S.) providing a horizontal reference line. We then normalized the microtopography relative to the elevation of groundwater probe location at micrometeorology station. Microtopography of the total 30 microsites ranges from −7.5 to 20 cm. All microsites were classified to three groups corresponding to the HIGH, MID, and LOW microsites of the automated measurements. Survey data collected from the same type of microsites on the same day were combined statistically. Seasonal variation of the mean survey R_s was then compared to that of automated measurements.

2.5. Model Development

[18] Models were developed separately for flooded and nonflooded conditions due to the distinct phase shift and different mechanisms of R_s. For R_s under flooded conditions, we used T_s as the only independent driver. For R_s under nonflooded conditions, the conventional Q_{10} model (equation (1)) was used as the backbone, in which R_b, the basal respiration, is the respiration rate at base temperature (T_b), and Q_{10}, the indicator for temperature sensitivity, is the change in respiration rate caused by change in temperature by 10°C [*Luo and Zhou*, 2006]. We evaluated WTD effects on R_s through R_b and Q_{10} in the conventional Q_{10} model. If they were related to WTD, we then used WTD functions

for these two parameters to involve the WTD effects into the Q_{10} model (equation (2)).

$$R_s = R_b Q_{10}^{\frac{T_s - T_b}{10}} \qquad (1)$$

$$R_s = f_{R_b}(\text{WTD}) \left[f_{Q_{10}}(\text{WTD}) \right]^{\frac{T_s - T_b}{10}} \qquad (2)$$

where $f_{R_b}(\text{WTD})$ and $f_{Q_{10}}(\text{WTD})$ represent R_b and Q_{10} as the function of WTD.

2.5.1. Nonflooded Model

[19] The basal respiration is usually derived by regression as a model parameter, but it can also be an observable term by definition [*Yuan et al.*, 2011]. With R_b defined as the respiration rate at T_b, it can be used to evaluate the response of R_s to other potentially confounding factors as the temperature effect is excluded. With the confounding factors accounted for in R_b, the uncertainty could be decreased in the estimation of Q_{10}, which would arguably better represent the intrinsic temperature sensitivity [*Davidson and Janssens*, 2006; *Mahecha et al.*, 2010; *Reichstein et al.*, 2005; *Sampson et al.*, 2007].

[20] To evaluate the relationship between R_b and WTD in our forested wetland, we set T_b at 24°C to obtain the broadest range of WTD, which is higher than the mean temperature during the study period (19°C). The R_s with the range of temperatures constrained to within ±0.5°C, i.e., 23.5–24.5°C, were then separated out as R_b data. With the data in a narrow range of temperature and the widest coverage of WTD, the relationship between R_b and WTD (i.e., $f_{R_b}(\text{WTD})$) was analyzed. Over the T_s range of 1°, R_s did not exhibit any pattern with temperature, whereas the variation with WTD exhibited a strong response (Figure 3). There was a pattern of increasing R_s as WTD dropped from 0 to −10 or −20 cm (varied by microsites) with nearly constant R_s at deeper WTD. As this pattern resembled the saturating pattern of Michaelis-Menten reaction [*Davidson et al.*, 2006, 2012; *Johnson and Goody*, 2011], we simulated the dependence of R_b on WTD as (equation (3)):

$$R_b = f_{R_b}(\text{WTD}) = \frac{V_{\max}\text{WTD}}{K_m + \text{WTD}} \qquad (3)$$

where $V_{\max}$ is the maximum R_b rate at T_b, and K_m the water depth at half maximum R_b.

[21] For quantifying the WTD effects on temperature sensitivity of R_s, data were binned by WTD in 5 cm intervals when WTD was shallower than 30 cm below ground (i.e., from −30 cm up to ground level). The interval was set greater when WTD was deeper due to the limited sample size. We assumed that T_s was the primary driver of R_s within a given WTD class and estimated Q_{10} according to conventional Q_{10} model (equation (1)). Due to the interdependence between R_b and Q_{10} [*Janssens and Pilegaard*, 2003], two methods were used to derive Q_{10} of each group of data: (i) R_b was calculated with $f_{R_b}(\text{WTD})$ first, and only Q_{10} was estimated by regression; and (ii) both R_b and Q_{10} were estimated by regression. Ultimately, the WTD was averaged for each group and used to analyze the relationship between Q_{10} and WTD (i.e., $f_{Q_{10}}(\text{WTD})$). The pattern of Q_{10} varying

Table 1. Comparison of Q_{10} (Mean ± SE) Estimated From Two Methods for Soil CO_2 Effluxes (R_s) With Different Water Table Depth (WTD) at HIGH Microsite in a Coastal Plain Forested Wetland in the Southeastern U.S.

WTD Range[a] (cm)	Mean WTD (cm)	Observed T_s Range (°C)	Method (i)[b]			Method (ii)[c]		
			R_b	Q_{10}	RMSE[d]	R_b	Q_{10}	RMSE
−45 to −30	−34.5	22.2–25.4	9.12	0.49 ± 0.08	2.99	10.80 ± 0.09	1.51 ± 0.20	2.57
−30 to −25	−27.2	15.1–25.5	8.93	1.96 ± 0.12	2.64	8.33 ± 0.08	1.55 ± 0.10	2.59
−25 to −20	−22.4	15.1–24.8	8.75	2.13 ± 0.07	3.03	8.64 ± 0.10	2.07 ± 0.09	3.03
−20 to −15	−17.7	11.7–25.5	8.49	2.07 ± 0.04	2.61	9.56 ± 0.09	2.54 ± 0.07	2.55
−15 to −10	−12.7	6.7–24.4	8.05	3.82 ± 0.05	1.29	9.76 ± 0.09	4.66 ± 0.07	1.21
−10 to −5	−7.5	3.3–24.1	7.14	5.20 ± 0.16	0.76	8.36 ± 0.04	6.37 ± 0.23	0.65

[a]At each WTD class, it was assumed that soil temperature (T_s) was the primary driver of soil respiration.
[b]R_b was calculated first with $f_{R_b}(\text{WTD}) = \frac{V_{\max}\text{WTD}}{K_m + \text{WTD}}$, and then Q_{10} was estimated from conventional Q_{10} model: $R_s = R_b Q_{10}^{\frac{T_s - 24}{10}}$. When estimating Q_{10}, R_b was set as constants.
[c]Both R_b and Q_{10} were estimated from conventional Q_{10} model.
[d]Root mean square error.

with WTD was mostly consistent between the two methods despite the estimation uncertainty (Table 1). We simplified the dependence of Q_{10} on WTD as an exponential function:

$$Q_{10} = f_{Q_{10}}(\text{WTD}) = \beta_1 \exp[\beta_2(\text{WTD} + 10)] \qquad (4)$$

where β_1 is Q_{10} at WTD = −10 cm and β_2 is a fitted WTD-effect parameter. The β_1 indicates that R_s at WTD = −10 cm increases ($\beta_1 - 1$) times for every 10° rise in temperature. The β_2 means that per unit decrease in WTD (i.e., −1 cm) would cause Q_{10} to decrease by $[1 - \exp(\beta_2)]$.

[22] By combining equations (3) and (4), we derived the aerobic R_s model accounting for the effect of WTD as equation (5). The model was then fitted to the continuous nonflooded data sets at each microsite. We named it "nested Q_{10} model" because the functions for the two parameters were nested into the conventional Q_{10} model. The coefficients were derived by the nonlinear least squares method with Levenberg-Marquardt algorithm [*Seber and Wild*, 2003]. All computations were done with MATLAB 7.11 R2010b (The MathWorks Inc., U.S.).

$$R_s = \frac{V_{\max}\text{WTD}}{K_m + \text{WTD}} \{\beta_1 \exp[\beta_2(\text{WTD} + 10)]\}^{\frac{T_s - 24}{10}} \qquad (5)$$

2.5.2. Performance Comparison Between Models

[23] We compared performance of the nested Q_{10} model with those of the conventional Q_{10} (equation (1), T_b = 24°C) and multiplicative model (equation (6)) and evaluated the derived temperature sensitivity with or without accounting for the WTD effect. The multiplicative model can be viewed as a specific form of nested Q_{10} model, i.e., only R_b is dynamic and Q_{10} is constant, and is sometimes used as an improved Q_{10} model [*Davidson et al.*, 1998; *Tang et al.*, 2005b].

$$R_s = R_b \exp[\beta(\text{WTD} + 10)]Q_{10}^{\frac{T_s - 24}{10}} \qquad (6)$$

[24] Mean square error (MSE, equation (7)) was used to compare the model performance between all the three models, in which the number of drivers and parameters differs. In addition, Akaike's information criterion (AIC, equation (8)) was calculated for the multiplicative model and the nested model to assess if the latter is truly better or an overfit of the

data by introducing an additional parameter [*Anderson et al.*, 2000; *Motulsky and Christopoulos*, 2004]. The coefficient of determination (R^2, equation (9)) was also calculated to demonstrate the explained variation of R_s by the fitted model with identified driver(s) [*Kvalseth*, 1985].

$$\text{MSE} = \frac{\text{RSS}}{n - K} \qquad (7)$$

$$\text{AIC} = n \ln\frac{\text{RSS}}{n} + 2K \qquad (8)$$

$$R^2 = 1.0 - \frac{\text{RSS}}{\text{TSS}} \qquad (9)$$

where RSS represents the residual sum of squares and TSS the total sum of squares. n is the number of observations, and K is the number of parameters.

2.5.3. Modeling With Two Data Sets

[25] One of the uncertainties of modeling R_s with 30 min data is from the variability at different time scales under which the factors influencing R_s may vary [*Baldocchi et al.*, 2001; *Riveros-Iregui et al.*, 2007]. We hypothesized that the model fit would increase with daily data due to temperature- or WTD-independent variability in the diel cycle. To test this hypothesis, we sorted out the dates when all 48 half-hourly records were present and had passed the quality assurance criteria and calculated daily integrated R_s. Similarly to the 30 min data, we fitted equations (1), (5), and (6) to daily integrated R_s data. MSE, AIC, and R^2 were calculated to compare model performance as well.

2.5.4. Flooded Model

[26] We tested two temperature-dependent models for modeling flooded CO_2 efflux: a diffusion model from aquatic ecosystems [*Casper et al.*, 2000; *Maberly*, 1996] and a simple quadratic equation derived from regression between observed flooded CO_2 efflux and T_s. Performance was similar between the two models; we then chose the simpler quadratic equation. The regression was done separately for three microsites (Table 2).

2.6. Gap Filling and Estimation of Annual Total Soil CO_2 Efflux

[27] Missing 30 min flux data were gap filled separately for nonflooded and flooded periods. Nonflooded CO_2 efflux was gap filled with the nested model (equation (5)). During flooded periods, two criteria were used to fill the missing values. (i) If

Table 2. Quadratic Models for Modeling Soil CO_2 Effluxes at Three Microsites (HIGH, MID, and LOW) With Soil Temperature (T_s) During Flooded Periods in a Coastal Plain Forested Wetland in the Southeastern U.S.

	Model	R^2	p Value	Sample Size
HIGH	$R_s = -0.48 + 0.16T_s - 0.0047T_s^2$	0.0213	<0.001	1252
MID	$R_s = -0.06 + 0.06T_s - 0.0013T_s^2$	0.1669	<0.001	6090
LOW	$R_s = -1.02 + 0.19T_s - 0.0052T_s^2$	0.0152	<0.001	2858

there were valid measurements during a given flooding day, the missing flux values were simply set equal to the arithmetic mean of existing observed fluxes because of minimal diurnal fluctuation in flooded fluxes. (ii) If there were no measurements during a day or continuous days, the missing values were filled with the quadratic equation (equations in Table 2). The total annual CO_2 loss was estimated as the sum of CO_2 efflux during nonflooded and flooded periods. The nonflooded CO_2 efflux was also predicted based on T_s and/or WTD with the three models.

3. Results

3.1. Seasonal CO_2 Efflux and Spatial Heterogeneity

[28] The seasonal pattern of R_s appeared consistently between automated and survey measurements (Figure 2). Pronounced differences between microsites were present throughout the year in automated measurements but decreased in magnitude during summer months in the survey measurements. In general, the site was driest during summer (June, July. and August, Figure 1b) with WTD below surface (mean WTD = −10 cm in summer 2010) and had the greatest CO_2 release of the year. During summer the individual peak efflux reached 21.0 μmol CO_2 m^{-2} s^{-1} and the mean value at HIGH microsite was 8.5 ± 3.7 (mean ± SD) μmol CO_2 m^{-2} s^{-1}. The mean CO_2 flux at MID and LOW microsites was 5.7 ± 3.1 and 3.8 ± 1.6 μmol CO_2 m^{-2} s^{-1}, respectively. The maximum daily total CO_2 loss was 12.9, 9.8, and 6.0 g CO_2-C m^{-2} d^{-1} in HIGH, MID, and LOW microsites, respectively. Rain events during summer caused temporary flooding, resulting in uniformly low CO_2 efflux, with no significant difference between the three microsites. Flooded CO_2 flux during summer averaged 0.6 μmol CO_2 m^{-2} s^{-1} and ranged from 0.1 to 3.5 μmol CO_2 m^{-2} s^{-1}.

[29] Most of the soil surface was submerged during autumn (September, October, and November, mean WTD = 14 cm in 2010) and winter (December, January, and February, mean WTD = 12 cm). CO_2 flux was generally less than 1.0 μmol CO_2 m^{-2} s^{-1} during this time. The flux during winter was the lowest due to the combination of flooding and low temperature and averaged about 0.3 μmol CO_2 m^{-2} s^{-1} at all microsites. The water table drew down gradually in winter and the following spring (March, April, and May; mean WTD = 2 cm in spring 2011). The HIGH microsite was first exposed to the air in spring, and as a result CO_2 flux increased despite the similar temperatures in spring and autumn. The low-lying microsites were still submerged during spring and had comparable magnitude of CO_2 flux between spring and autumn. The respective mean CO_2 efflux at HIGH microsite during spring and autumn was 3.2 and 0.9 μmol CO_2 m^{-2} s^{-1}, respectively, whereas at MID it was 0.8 and 0.6 μmol CO_2 m^{-2} s^{-1}.

3.2. Water Table Fluctuation and Temperature Effects on Soil Respiration

[30] Water table fluctuation determines the transition between flooded and nonflooded status of soil, and R_s responded to the change in status rapidly. Besides the seasonal variation associated with the hydroperiod, occasional precipitation events resulted in a temporarily flooded or near-flooded conditions and caused rapid decrease in R_s, e.g., the depressions in the clear area of Figure 2.

[31] Under nonflooded conditions, the R_s-WTD relationship (with temperature effect included, Figures 4d–4f) was similar to the R_b-WTD one (with temperature effect not included, Figures 3d–3f), implying the confounding effects between T_s and WTD. The evident dichotomy in both R_s-T_s and R_s-WTD relationships at HIGH microsite (Figures 4a and 4d) indicates the effects independent of one another between the two drivers. The R_s-T_s relationship generally exhibited an exponential pattern, but the WTD imposed additional effects on the R_s-T_s relationship (Figure 4a). For example, the T_s was 21.5°C during a period in July of both 2009 and 2010, while the WTD at HIGH microsite was −3 and −25 cm respectively. Correspondingly, the R_s was 1.5 μmol C m^{-2} s^{-1} in 2009 and 6.8 μmol C m^{-2} s^{-1} in 2010. Likewise, the T_s also resulted in the bifurcation in R_s-WTD relationship (Figure 4d). The WTD during some period in summer 2009 was at the same level as that during winter 2010, i.e., −7 cm, while the T_s was 23.7 and 4.7°C resulting in the R_s difference between 7.7 and 0.4 μmol C m^{-2} s^{-1}.

3.3. Modeled Temperature Sensitivity and Water Table Depth Effects

[32] The difference in Q_{10} among the three microsites, determined by β_1 and β_2 in the nested Q_{10} model, varied with WTD (Table 3 and Figures 5c and 5f). Higher β_1 implies higher Q_{10} at WTD = −10 cm, and higher β_2 implies faster
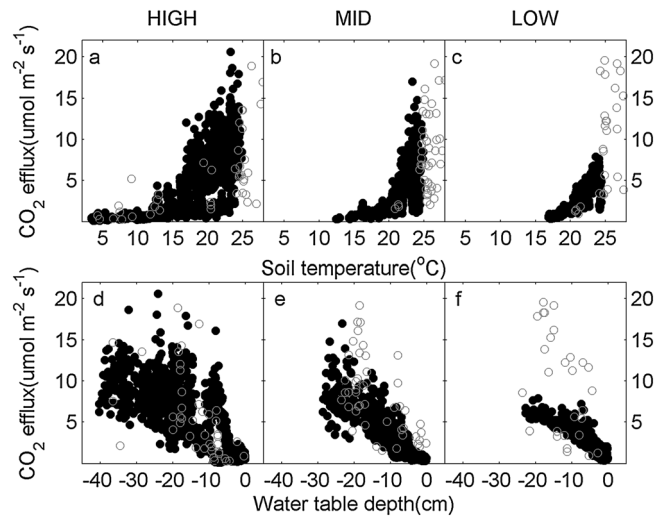

Figure 4. Relationship (a–c) between nonflooded soil CO_2 efflux (R_s) and soil temperatue at 5 cm depth and (d–f) between R_s and water table depth at HIGH (in Figures 4a and 4d), MID (in Figures 4b and 4e), and LOW (in Figures 4c and 4f) microsites. Black dots represent automated measurements, and grey circles represent survey measurements.

Table 3. Parameters (Mean ± SE) of Three Soil Respiration Models (the Conventional Q_{10} Model, the Multiplicative Model, and the Nested Q_{10} Model) From Regression With 30 min Soil CO_2 Efflux Data and Daily Soil CO_2 Efflux Data

Model Parameters	Unit	Microsite			
		HIGH	MID	MID-2[a]	LOW
30 min Soil CO_2 Efflux Data					
		Conventional Q_{10} model			
R_b	$\mu mol\,CO_2\,m^{-2}\,s^{-1}$	10.02 ± 0.05	6.97 ± 0.05		4.94 ± 0.03
Q_{10}		5.14 ± 0.10	11.48 ± 0.55		11.03 ± 0.47
MSE[b]		7.5435	5.4522		2.0875
R^2		0.6225	0.5195		0.6243
		Multiplicative model			
R_b	$\mu mol\,CO_2\,m^{-2}\,s^{-1}$	7.33 ± 0.06	5.12 ± 0.05		4.49 ± 0.02
Q_{10}		3.09 ± 0.05	4.57 ± 0.18		5.27 ± 0.16
β		−0.0217 ± 0.0004	−0.0447 ± 0.0008		−0.0425 ± 0.0006
MSE		5.6211	2.8923		0.4500
AIC[c]		18644	5617		−2718
R^2		0.7187	0.7452		0.8590
		Nested Q_{10} model			
V_{max}	$\mu mol\,CO_2\,m^{-2}\,s^{-1}$	13.58 ± 0.13	19.59 ± 0.53	11[a]	7.63 ± 0.08
K_m	cm	−7.2 ± 0.3	−26.5 ± 1.23	−8.1 ± 0.1	−5.4 ± 0.2
β_1		3.63 ± 0.08	5.27 ± 0.21	6.07 ± 0.23	3.91 ± 0.12
β_2	m^{-1}	0.0533 ± 0.0022	0.1651 ± 0.0060	0.06[a]	0.0673 ± 0.0058
MSE		3.5597	1.8612	2.4750	0.2761
AIC		13713	3288	4793	−4381
R^2		0.8219	0.8360	0.7819	0.9135
Sample Size		10797	5286		3407
Daily Soil CO_2 Efflux Data					
		Conventional Q_{10} model			
R_b	$g\,CO_2\text{-}C\,m^{-2}\,d^{-1}$	10.58 ± 0.38	7.55 ± 0.37		4.77 ± 0.30
Q_{10}		3.65 ± 0.57	12.94 ± 4.31		9.06 ± 3.64
MSE		4.9281	3.2008		1.0448
R^2		0.6905	0.6928		0.5918
		Multiplicative model			
R_b	$g\,CO_2\text{-}C\,m^{-2}\,d^{-1}$	8.13 ± 0.53	5.47 ± 0.36		4.82 ± 0.17
Q_{10}		2.57 ± 0.37	4.79 ± 1.27		5.62 ± 1.41
β		−0.0162 ± 0.0032	−0.0389 ± 0.0055		−0.0500 ± 0.0055
MSE		3.6569	1.4502		0.2900
AIC		114.45	24.85		−41.69
R^2		0.7731	0.8633		0.8900
		Nested Q_{10} model			
V_{max}	$g\,CO_2\text{-}C\,m^{-2}\,d^{-1}$	13.11 ± 0.91	19.97 ± 2.26	11[a]	8.21 ± 0.68
K_m	cm	−6.1 ± 1.9	−26.4 ± 5.2	−7.4 ± 0.6	−5.9 ± 1.1
β_1		3.64 ± 0.76	5.10 ± 0.79	6.39 ± 1.30	4.33 ± 1.04
β_2	m^{-1}	0.0601 ± 0.0197	0.2007 ± 0.0250	0.065[a]	0.0690 ± 0.0473
MSE		2.1656	0.3229	0.9384	0.1151
AIC		70.36	−62.83	−1.79	−74.09
R^2		0.8672	0.9701	0.9099	0.9577
Sample Size		86	59		36

[a]In nested Q_{10} model, the values of V_{max} and β_2 were manually set.
[b]Mean square error.
[c]Akaike's information criterion.

change of Q_{10} with WTD. Both β_1 and β_2 were lower at HIGH than at LOW microsite, and as a result Q_{10} was lower at HIGH than LOW microsite when WTD was relatively shallow (from −5 to −15 cm) but higher when WTD was deeper. When the WTD decreased from −5 to −15 cm, Q_{10} decreased from 4.7 to 2.8 at HIGH microsite, whereas it decreased from 5.5 to 2.8 at LOW microsite. When the WTD decreased further from −15 to −25 cm, the Q_{10} decreased from 2.8–1.6 and 2.8–1.4 at HIGH and LOW microsite, respectively (Figure 5f).

[33] The parameters in the nested model were much higher at MID than at the other two microsites (Table 3). While this modeled greater sensitivity to environmental drivers might be real at MID than other microsites, it is more likely that the weakly defined asymptotic relationship between R_b and WTD due to limited WTD range (Figure 3e) led to parameter convergence at unrealistic values. To aid model convergence at the MID microsite, we interpolated the V_{max} and β_2 parameter values based on the HIGH and LOW microsites ($V_{max} = 11\,\mu mol\,C\,m^{-2}\,s^{-1}$ and $\beta_2 = 0.06$ m^{-1}, MID-2 in
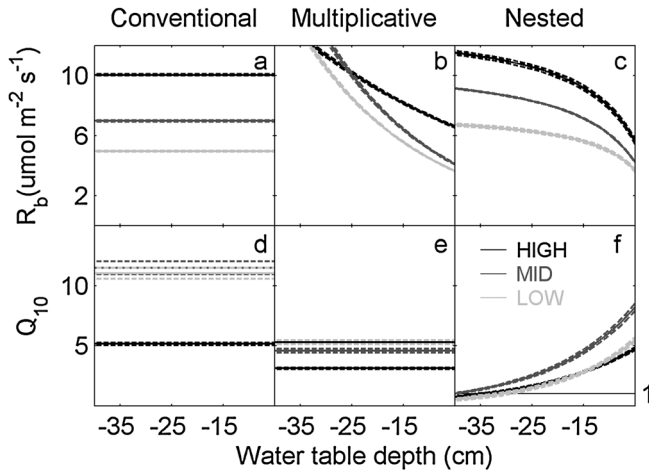
Figure 5. Comparison of relationships (a–c) between water table depth and basal respiration (R_b) and (d–f) between water table depth and Q_{10} simulated by the three models: the conventional Q_{10} model (in Figures 5a and 5d); the multiplicative model (in Figures 5b and 5e); and the nested model (in Figures 5c and 5f). Solid line represents mean value, and dashed line is standard error of the parameters.

Table 3). With these two parameter corrections, the K_m was estimated to be 8 cm below ground and β_1 to be 6.1.

[34] In contrast to the dynamic trends of spatial difference reflected in parameters of the nested model, the trends resulting from the conventional Q_{10} and multiplicative models were fixed and differed between the two models (Table 3 and Figures 5a, 5b, 5d, and 5e). The HIGH microsite had the lowest Q_{10} and the highest R_b according to all models throughout most of the year. The Q_{10} of the conventional Q_{10} model was not significantly different between MID and LOW microsites, while from the multiplicative model the MID microsite had lower Q_{10} and more negative β, i.e., lower temperature sensitivity but greater WTD effect ($p < 0.01$).

3.4. Comparison of Model Performances and Two Data Sets

[35] The conventional Q_{10} model captured 50–60% of the R_s variation with variability in T_s. The multiplicative model improved the performance by accounting for the effects of WTD and increased R^2 to 70–80%. The nested model increased the simulated variation by an additional 4–10%. For MID microsite, the R^2 decreased 5% with the manually set values in the nested model but was still high at 78% with increases of 26% and 4% relative to the conventional Q_{10} and multiplicative models, respectively. The lower MSEs and AICs of the nested model with both the 30 min and daily data also indicated that the nested model performed better than the conventional models, even as penalized for the greater number of parameters (Table 3).

[36] The modeled driver effects further exhibited the different performance from the three models with static or dynamic parameters (Figure 6). The conventional Q_{10} model derived the smooth exponential curve of R_s-T_s relationship (Figure 6a), and the seemingly good simulation of R_s-WTD relationship disclosed the partial confounding WTD effects in temperature effects (Figure 6d). However, it could not simulate the temperature and WTD effects independent of

each other. Despite the increased R^2 and decreased MSE compare to the conventional Q_{10} model (Table 3), the multiplicative models also did not describe the relationship well (Figure 6b). The nested Q_{10} model simulated the bifurcations well in both R_s-T_s (Figure 6c) and WTD-R_s (Figure 6f) relationships.

[37] Differences in model parameters among the microsites were consistent at both 30 min and daily timescale, but improvement in model performance differed by microsite (Table 3). Through the comparison of MSE, AIC, R^2, and the distribution of residuals, modeling with daily data performed better at MID and LOW compared to HIGH microsites. The R^2 of 30 min data at LOW microsite was 91%, while the daily data reached 96%, indicating that the
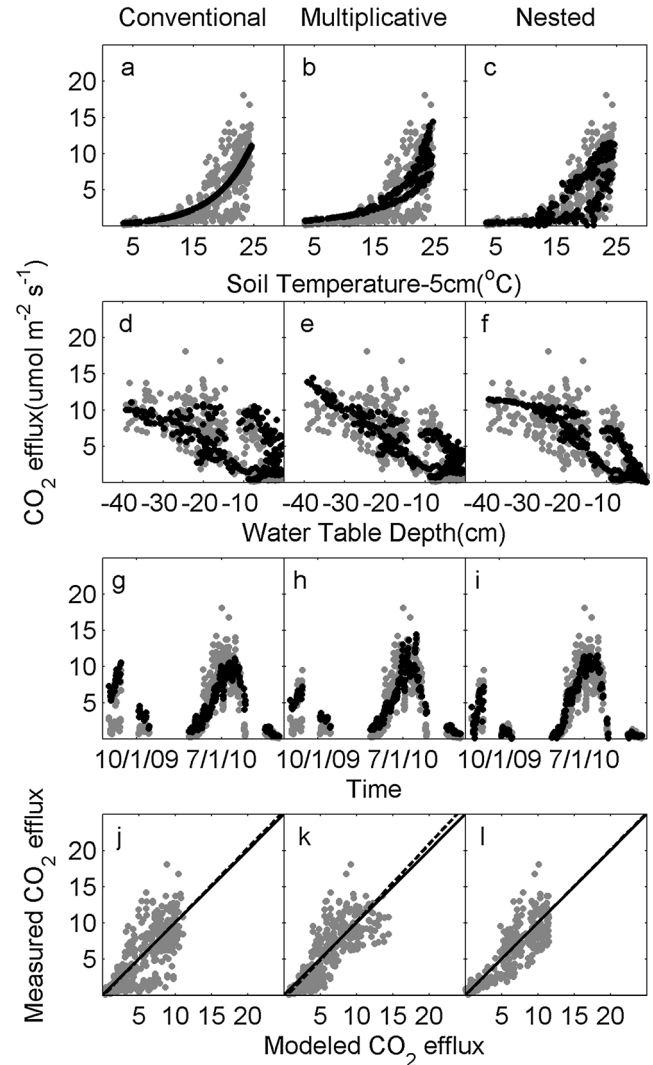

Figure 6. Comparison of modeled (black dots) and measured (grey dots) driver effects on soil CO_2 efflux (R_s) at HIGH microsite by (a, d, g, and j) the conventional Q_{10} model, (b, e, h, and k) the multiplicative model, and (c, f, i, and l) the nested Q_{10} model. R_s-soil temperature relationship (in Figures 6a–6c); R_s-water table depth relationship (in Figures 6d–6f); R_s time series (in Figures 6g–6i); modeled R_s versus measured R_s with solid 1:1 line and dotted regression line (in Figures 6j–6l). Only part of data were shown.
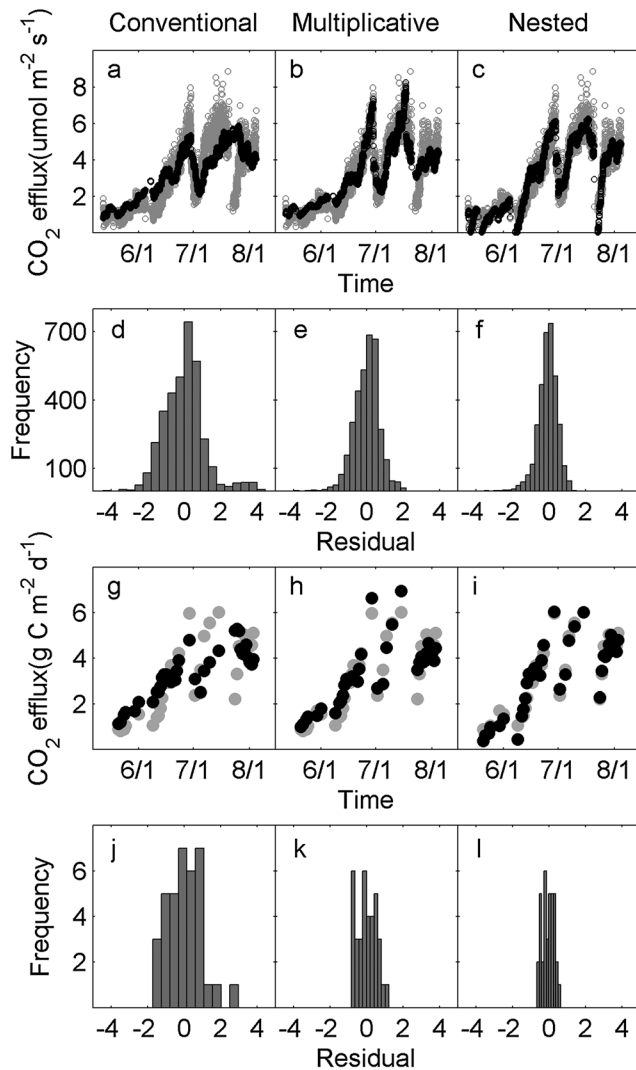
Figure 7. Comparison of modeled (black dots) and measured (grey dots) soil CO_2 efflux between the models using 30 min data set ((a–c) time series; (d–f) residual distribution) and daily data set ((g–i) time series; (j–l) residual distribution) from LOW microsite. Models include: the conventional Q_{10} model (in Figures 7a, 7d, 7g, and 7j), multiplicative model (in Figures 7b, 7e, 7h, and 7k) and the nested Q_{10} model (in Figures 7c, 7f, 7i, and 7l).

two environmental drivers can account for nearly all of the seasonal variation at this location (Table 3 and Figure 7). In contrast, at HIGH microsite the R^2 increased from 82% to 87%, with 13% still unaccounted for (Table 3). In other words, the diel variability independent of T_s and WTD was greatest at the HIGH microsite.

3.5. Estimation of Annual Total Soil CO_2 Efflux

[38] With the gaps filled separately for nonflooded and flooded records, i.e., the nested model for nonflooded and the quadratic temperature-response equation for flooded, the annual soil CO_2 efflux at HIGH microsite was estimated at 1325 (95% CI: 1291–1365) g C m^{-2} yr^{-1} in 2010, while MID and LOW microsites released an estimated 621 (555–710) and 430 (319–694) g C m^{-2} yr^{-1}, respectively. The nonflooded

periods contributed most of the CO_2-C loss annually, ranging from 72 to 97% at the different microsites (Table 4).

[39] The difference of cumulative R_s between 2009 and 2010 was attributable to the differences in the number of flooding and nonflooding days between the two years. From July to December, the percentage of nonflooding days at HIGH microsite was 51% (approximately 185 days) in 2009 and 85% (approximately 305 days) in 2010, which resulted in 308 and 704 g C m^{-2} of CO_2 efflux. At MID and LOW microsites, the R_s over the same period was approximately 2–3 times higher in the drier 2010 than in 2009 (Table 4).

[40] The prediction of CO_2 efflux during nonflooded periods differed markedly between the three models (Table 5). Generally, the conventional Q_{10} and multiplicative models overestimated R_s compared to the nested model. However, the difference between the models may have been exaggerated by the unequal data coverage between the years. For example, 87% of the data at HIGH microsite came from 2010, and only 13% came from 2009. Thus, it should perhaps not be a surprise that the annual fluxes estimated with the conventional model and the multiplicative model differed by as much 105% and 48% from that with the nested model in 2009. The annual estimates for 2010 by the three models were within 5% of each other.

4. Discussion

4.1. The Effect of Water Table Fluctuation on Seasonal Variation of Soil Respiration

[41] The bifurcation in R_s-T_s relationship at HIGH microsite demonstrates the seasonal hysteresis of R_s (Figures 4a and 8a), that is, the pattern that R_s responded differently to T_s in different seasons. At HIGH microsite, R_s was higher earlier in the growing season than later. This pattern was similar to the hysteresis observed in R_s in a boreal aspen forest and a mixed conifer and oak forest in California, which was attributed to high rates of fine-root production early in the growing season and/or the drought conditions during late summer [*Gaumont-Guay et al.*, 2006; *Vargas and Allen*, 2008]. The opposite pattern, documented in some other boreal and temperate forests, has been attributed to higher microbial activity due to deeper soil warming [*Drewitt et al.*, 2002; *Goulden et al.*, 1998; *Morén and Lindroth*, 2000; *Phillips et al.*, 2010]. In the current study, root growth and soil warming may both have contributed to the seasonal dynamics of R_s, but both are ultimately linked to WTD and flooding status (Figure 8d). The higher WTD (i.e., flooded conditions) during autumn resulted in the lower CO_2 efflux, and lower WTD (i.e., nonflooded conditions) during spring and summer corresponded to higher CO_2 efflux.

[42] The seasonal hysteresis pattern differed among the three microsites due to their elevation and associated hydrology. Compared with the HIGH microsite, the difference in R_s between spring and autumn at MID and LOW microsites was less pronounced as these microsites were flooded during both spring and summer (Figure 8).

[43] The WTD-driven regulation of R_s is associated with aeration, enzyme activity, and the composition of decomposer communities. While measuring biotic factors is beyond the scope of the current study, this association has been studied in other wetlands. For example, *Freeman et al.* [2001, 2004] suggested that peat decomposition in northern peatlands is

Table 4. Total Annual Carbon Efflux Estimation (Mean and 95% Confidence Interval, $g\,CO_2$-$C\,m^{-2}$) at HIGH, MID, and LOW Microsites in a Coastal Plain Forested Wetland in the Southeastern U.S. in 2009 and 2010

	Jul–Dec 2009			Jan–Jun 2010			Jul–Dec 2010			2010 Total		
	HIGH	MID	LOW	HIGH	MID	LOW	HIGH	MID	LOW	HIGH	MID	LOW
Nonflooded periods												
Percentage of days (%)	50.8	0	0	77.4	37.6	26.8	84.8	27.8	25.1	81.1	21.7	17.2
Gap-filled mean	308	0	0	579	187	106	704	326	204	1283	513	311
95% CI-Lower	303	0	0	578	186	106	701	326	203	1279	512	309
95% CI-Upper	314	0	0	581	187	107	706	326	205	1287	513	312
Flooded periods												
Percentage of days (%)	49.2	100	100	22.6	62.4	73.2	15.2	72.2	74.9	18.9	78.3	82.8
Gap-filled mean	65	102	109	19	39	47	23	68	72	42	108	119
95% CI-Lower	31	37	32	4	15	8	9	29	2	12	43	10
95% CI-Upper	102	172	246	40	83	175	38	113	207	77	196	382
Total												
Mean	374	102	109	598	226	154	727	394	276	1325	621	430
95% CI-Lower	333	37	32	582	201	114	710	355	205	1291	555	319
95% CI-Upper	416	172	246	620	270	282	744	440	412	1365	710	694

limited by a single enzyme, phenol oxidase, due to oxygen limitation. *Jaatinen et al.* [2007] found that the microbial communities changed significantly following water table fluctuation in a southern boreal peatland.

4.2. The Effect of Time Scale, Spatial Variation, and Association With Plant Activity

[44] As expected, model fit increased when applied to daily data, even though the smaller sample size led to higher uncertainty of parameter estimates (Table 3 and Figure 7). The results were consistent with the view that eliminating the diel variation would improve the simulation of seasonal variation and suggested that T_s and WTD fluctuations were the primary drivers of the seasonal cycle.

[45] Compared with some upland ecosystems where diel variation of R_s is related to high diel temperature variation [*Ruehr et al.*, 2010], the forested wetland had small diel variation in T_s due to the buffering influence of high water table.

For example, the daily range of T_s during the summer of 2010 was $0.54 \pm 0.17°C$ (mean $\pm$ SD), while the range of R_s at HIGH, MID, and LOW microsite was 8.0 ± 2.1, 5.7 ± 2.8, and $3.6 \pm 2.8\,\mu mol\,C\,m^{-2}\,s^{-1}$, respectively. The diel variation of WTD was also small with the daily range at $1.7 \pm 0.6\,cm$ excluding days with precipitation. The mismatch between the ranges of variability suggests that the diel variation in R_s was relatively independent of the T_s and WTD fluctuations and might be driven by other factors.

[46] The role of plant activity on R_s dynamics, which influences both autotrophic and heterotrophic respiration, has also been widely demonstrated in upland ecosystems [*Bahn et al.*, 2010; *Högberg and Read*, 2006; *Kuzyakov and Gavrichkova*, 2010]. Although the evidence is less clear in wetland ecosystems where the plants are acclimated to periodic inundation [*Lugo et al.*, 1990; *Mitsch and Gosselink*, 2007], we hypothesized that plant activity in wetlands, especially under nonflooded conditions, may play similar roles as in upland

Table 5. Comparison of Carbon Efflux Predictions (Mean and 95% Confidence Interval, $g\,CO_2$-$C\,m^{-2}$) by the Three Models (the Conventional Q_{10} Model, the Multiplicative Model, and the Nested Q_{10} Model) During Nonflooded Periods in 2009 and 2010

|	Jul–Dec 2009	Jan–Jun 2010			Jul–Dec 2010			2010 Total		
	HIGH	HIGH	MID	LOW	HIGH	MID	LOW	HIGH	MID	LOW
Percentage of data in the whole data set (%)	13.0	40.9	57.1	55.3	46.1	42.9	44.7	87.0	100	100
Conventional Q_{10} model										
Mean	651	460	202	115	832	331	185	1292	533	300
95% CI-Lower	644	451	196	112	821	326	182	1272	522	294
95% CI-Upper	659	469	208	119	843	336	188	1312	543	306
Multiplicative model										
Mean	468	525	205	118	825	328	215	1350	532	333
95% CI-Lower	460	517	200	116	813	323	212	1330	523	329
95% CI-Upper	477	534	209	120	836	332	217	1371	542	337
Nested Q_{10} model										
Mean	317	541	192	106	739	320	200	1279	513	307
95% CI-Lower	310	533	189	105	729	317	198	1262	506	303
95% CI-Upper	325	549	196	108	749	324	202	1297	520	310
Deviation from the nested model results										
Conventional Q_{10}	105.4%	−15.0%	5.2%	8.5%	12.6%	3.4%	−7.5%	1.0%	3.9%	−2.3%
Multiplicative	47.6%	−3.0%	6.8%	11.3%	11.6%	2.5%	7.5%	5.6%	3.7%	8.5%
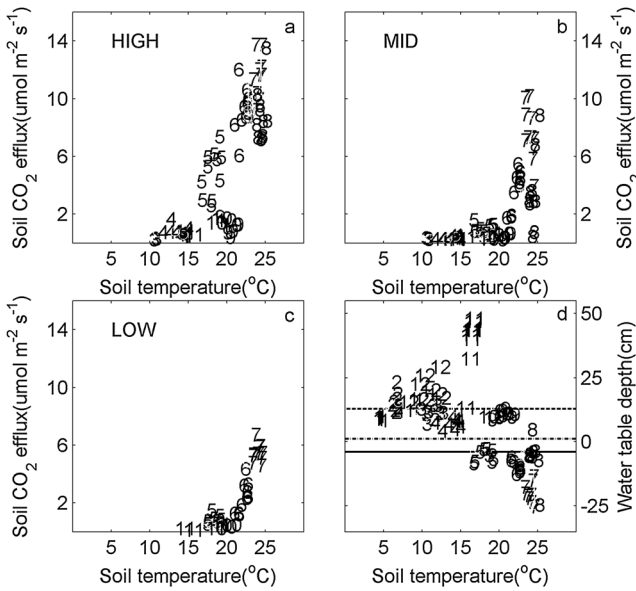
Figure 8. Relationship between soil CO_2 efflux (R_s) and drivers observed at HIGH, MID, and LOW microsites during 1 October 2009 to 30 September 2010 in a lower coastal plain forested wetland in the southeastern U.S. Numbers in the figure represent month. (a) R_s at HIGH microsite exhibited a clear seasonal hysteresis: higher rate during spring/summer because of nonflooded condition versus lower rate during autumn under flooded condition. (b and c) R_s at MID and LOW microsites did not show the same seasonal pattern as HIGH microsite, because the two low-lying sites were flooded during both spring and autumn. (d) Seasonal pattern of interaction between soil temperature and water table depth. Lines represent the elevation of three microsites relative to water table probe location (HIGH: dashed line; MID: dash dot line; LOW: solid line).

ecosystems. It has been found in various upland forests that diel R_s was related to the diel variation in photosynthetically active radiation or gross primary production, suggesting the main contribution of photosynthesis to diel R_s [*Liu et al.*, 2006; *Tang et al.*, 2005a]. Diel R_s dynamics are much less investigated in wetlands, but *Thomas et al.* [1996] observed in a peatland dominated by *Sphagnum* moss that a diel maximum CO_2 concentration in peats corresponded to minimum oxygen, reflecting the photosynthetic rates of surface vegetation. Plants in our forested wetland might contribute in different magnitude compared to the moss-dominated peatland and will be investigated in future studies.

[47] Furthermore, the spatial variation of R_s also provided us some insights on the role of plant activity on R_s dynamics in both diel and seasonal scale. Microsite-specific studies observed significant difference in diel and seasonal variation of R_s between microsites due to the vegetation distribution, in both dryland [*Cable et al.*, 2012; *Tang et al.*, 2005a] and wetland ecosystems [*Alm et al.*, 1997]. This is similar to the difference in R_s between HIGH, MID, and LOW microsites in our study. In wetlands, elevated microsites generally have higher root biomass and annual fine-root production than microsites in low-lying areas [*Jones et al.*, 1996; *Sullivan et al.*, 2008], which helps explain the increase in diel R_s variation along with the microtopographic gradient from LOW to HIGH microsites. It is also suggestive of the contribution of autotrophic

respiration to R_s at the diel scale. The small improvement of model performance at HIGH microsite with daily data may also indicate that plant activity is also a main contributor to seasonal variation, whereas at MID and LOW microsites the plant contribution was less significant (Table 3 and Figure 7).

4.3. Implication of Dynamic Temperature Sensitivity of Soil Respiration

[48] The change of Q_{10} with WTD (Figure 5f) likely resulted from the change in relative contribution of respiratory components [*Högberg*, 2010; *Zhou et al.*, 2010]. Plant litter decomposition generally respond quickly to changes in environmental conditions [*Lee et al.*, 2004] and might contribute most to R_s when water table was shallower, causing the higher Q_{10}. Given the spatial differences in microtopography and vegetation coverage at HIGH and LOW microsites, we expected the contribution of the autotrophic component to be higher at the HIGH microsite near the tree base. Thus, the smaller decline in Q_{10} at HIGH than LOW microsite with water table drawdown might suggest smaller suppression/sensitivity of autotrophic than heterotrophic respiration in this forested wetland.

[49] Previous studies that partitioned R_s and assumed constant response of respiratory components to temperature have given contradictory results [*Bond-Lamberty et al.*, 2011; *Boone et al.*, 1998; *Lavigne et al.*, 2003]. For example, *Boone et al.* [1998] showed a higher Q_{10} value of autotrophic respiration (4.6) than heterotrophic respiration (2.5) and integrated R_s (3.5) in a temperate hardwood forest. *Bond-Lamberty et al.* [2011] found that heterotrophic respiration ($Q_{10} = 2.1$) was more sensitive than integrated R_s ($Q_{10} = 1.8$) in a boreal black spruce plantation, implying the autotrophic respiration is less sensitive ($Q_{10} < 1.8$). The dynamic Q_{10} of integrated R_s in our study implied the two opposing patterns, which varied with WTD. Although we cannot simply make conclusions without further study of R_s partitioning, these dynamic parameters and spatial variation provided an intriguing possibility to clarify the inconsistency of results.

[50] The Q_{10}-WTD relationship also suggests that there exists a WTD below which $Q_{10} < 1$, i.e., R_s will begin to decrease with temperature. While there is a recognized temperature optimum of physiological processes [*Larcher*, 2003], and a negative T_s-R_s relationship has sometimes been reported [*Lellei-Kovács et al.*, 2011; *Mäkiranta et al.*, 2009; *Tang et al.*, 2005a], the possibility of $Q_{10} \leq 1$ is rarely considered in models. In the current study, only HIGH microsite had the records of WTD deeper than the modeled critical depth, i.e., about -35 cm. Although R_s was nearly constant with the increase of T_s at this relatively dry condition, the narrow temperature range (within 2.5°C) imposed large uncertainties. Further studies of drier conditions are needed to test the modeling of $Q_{10} < 1$ in wetlands.

4.4. Modeling Soil Respiration in a Forested Wetland

[51] The format of our nested model (equation (5)) is similar to several modified R_s models (either Q_{10} or Arrhennius models) in literature [*Mäkiranta et al.*, 2009; *Reichstein et al.*, 2002] but with different approach to derive dynamic parameters. In previous studies, several strategies have been adopted for capturing the seasonal hysteresis and combining the effects of multiple drivers. Most studies have used the residual method with three steps: (1) fitting temperature-only
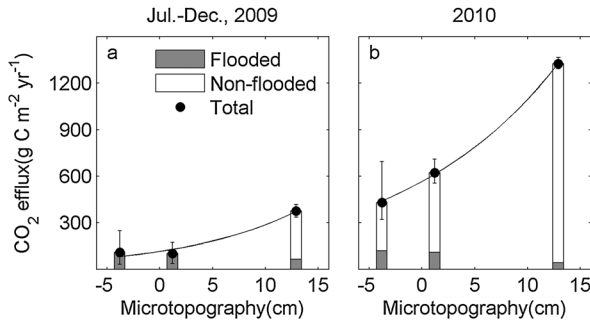
Figure 9. Relationship between microtopography and soil CO_2 efflux. Error bar represents the 95% confidence interval of total CO_2 efflux. Solid line represents the nonlinear regression with an exponential function: (a) $y = 114e^{0.091x}$ ($R^2 = 0.9697$, $p = 0.11$); (b) $y = 565e^{0.066x}$ ($R^2 = 0.9996$, $p = 0.01$).

models first (e.g., conventional Q_{10} model or Lloyd-Taylor model [*Lloyd and Taylor*, 1994]), (2) analyzing relationship between residuals and another driver (e.g., SWC), and (3) either adding or multiplying the additional-driver function to the temperature-only model, in which the residual pattern is generally site-specific [*Davidson et al.*, 1998; *Mäkiranta et al.*, 2009; *Savage and Davidson*, 2001; *Vincent et al.*, 2006]. There have also been studies applying the same model to different ecosystems without site-specific analysis [*Tang et al.*, 2005b; *Vargas and Allen*, 2008], which could also provide a better fit to observations like the multiplicative model we presented in this study. Few studies have constructed dynamic R_b and/or Q_{10} separately through specific data classification and combination into a single model [*Noormets et al.*, 2008; *Reichstein et al.*, 2002].

[52] While all these approaches are empirical in nature, the third group derives the relationships of model parameters with secondary drivers directly from observations, whereas the residual method is based on indirect statistical results. The application of the third method has historically been limited by measurement technology and sample size, but the deployment of automated measuring systems is currently reducing that limitation [*Carbone and Vargas*, 2008; *Savage and Davidson*, 2003]. The dynamic R_b and Q_{10} in the current study were derived through data classification, reducing the statistical influence. In spite of the uncertainties related to limited data at some WTD ranges, we conclude these functions performed well in characterizing our wetland ecosystem.

[53] With the M-M equation derived for R_b, the nested Q_{10} model was similar to the Dual Arrhenius and M-M kinetics (DAMM) model developed by *Davidson et al.* [2012]. In terms of the mathematical formulation, the subterms in our nested model can be rearranged and transformed to the format of DAMM model as (equation (10)):

$$R_s = \left(V_{max} \{\beta_1 \exp[\beta_2(\mathrm{WTD} + 10)]\}^{\frac{T_s - 24}{10}} \right) \times \frac{\mathrm{WTD}}{K_m + \mathrm{WTD}} \quad (10)$$

[54] The definition of some parameters in the nested model, e.g., the V_{max} (the maximum R_b at T_b), is equivalent to the pre-exponential factor (α_{Sx}, a parameter to define the maximum

velocity of the enzymatic reaction) in the DAMM model [*Davidson et al.*, 2012]. Some differences between the two models were associated with the limited factors we measured in the current study, for example, the WTD in our nested model versus the substrate and oxygen concentration in the DAMM model. However, WTD implicitly regulates the soil water content, oxygen, and substrate availability in wetlands [*Freeman et al.*, 2001; *Wheeler*, 1999], and from this point of view, our modeling study can be viewed as analogous to the DAMM model with some site-specific modification for a wetland ecosystem.

4.5. Importance of Microtopography in Estimating Soil CO_2 Efflux

[55] The observed spatial variation of R_s and associated microtopography heterogeneity led to our hypothesis that contribution from respiratory components varies between microsites. While microtopography was used as an indicator to characterize the spatial heterogeneity of belowground conditions in this forested wetland, the factors directly driving the variant contributions to R_s and their relationships with microtopography are uncertain, such as root biomass and production, redox potential, nutrients, etc. Measuring these factors is still a great challenge in forested wetlands, but several previous studies have suggested the significant influence of microtopography on these factors [*Ehrenfeld*, 1995; *Jones et al.*, 1996, 2000].

[56] However, the range of 430–1320 g C m^{-2} yr^{-1} observed at various microsites (Table 4) highlights the need for spatially explicit estimates of R_s when scaling point data to the stand scale to estimate ecosystem C balance. Such high spatial variation of R_s has been documented in other wetland ecosystems [*Alm et al.*, 1999; *Jauhiainen et al.*, 2005; *Luken and Billings*, 1985]. Despite the small sample size and associated uncertainty, the three microsites exhibited an exponential relationship between microtopography and R_s, with different magnitude between wet (2009) and dry (2010) years (Figure 9). While further long-term study with better coverage of microtopography variability is needed to test the exponential relationship, this preliminary result may help improve our estimation of R_s in wetland ecosystems with typical microtopographic variation. It also presents the possibility to quantify interannual variation of R_s at the ecosystem scale as the coefficients in the R_s-microtopography relationship are associated with climatic conditions.

[57] The annual soil CO_2 efflux at MID and HIGH microsites (Table 4) were similar to those reported for nearby pocosin and gum swamp ecosystems in North Carolina (672–1086 g C m^{-2} yr^{-1}) [*Bridgham and Richardson*, 1992] and a freshwater marsh in Louisiana (618 g C m^{-2} yr^{-1}) [*Smith et al.*, 1983]. The smaller flux at LOW microsite was similar to the salt marsh in the same study from Louisiana (418 g C m^{-2} yr^{-1}). Compared with upland systems, the magnitude of annual soil CO_2 efflux at HIGH, MID, and LOW microsite in 2010 were comparable with average soil CO_2 efflux of tropical evergreen broadleaf forest (1540 g C m^{-2} yr^{-1}), boreal deciduous broadleaf (650 g C m^{-2} yr^{-1}), and boreal evergreen needleleaf forest (360 g C m^{-2} yr^{-1}), respectively [*Gower*, 2003].

[58] Given the areal contribution of the different microtopographic positions in the landscape, 60% in HIGH, 23% in MID, and 17% in LOW, we estimated the site-average soil CO_2 efflux at 1015 g C m^{-2} yr^{-1} with 95% confidence interval

of 960 to 1103 $g\,C\,m^{-2}\,yr^{-1}$ in 2010, of which 93% was released during nonflooded periods. This site-average soil CO_2 efflux was much higher than that reported for northern wetlands and similar to some tropical wetlands. For example, the annual estimate is more than 2 times of the soil CO_2 flux at the wetlands at Harvard and Howland Forests (370–$480\,g\,CO_2$-$C\,m^{-2}\,yr^{-1}$) in northeast U.S. [*Savage and Davidson*, 2001], 2–4 times higher than those at a southern boreal peatland of Finland (220–$320\,g\,CO_2$-$C\,m^{-2}\,yr^{-1}$) [*Alm et al.*, 1999] and 5–10 times higher than at a subarctic peatland (80–$180\,g\,CO_2$-$C\,m^{-2}\,yr^{-1}$) [*Moore*, 1986] but similar to a tropical peat swamp forest in Indonesia (900–$1100\,g\,CO_2$-$C\,m^{-2}\,yr^{-1}$) [*Jauhiainen et al.*, 2005]. As 2010 was a dry year in the study area, the soil CO_2 efflux estimation may be higher than the long-term average, but this also indicates a potential for high C losses from wetland soils under drier conditions.

5. Conclusions

[59] Soil CO_2 efflux (R_s) in the forested wetland varied more than twofold as a function of microtopographic position, as measured over a 17 month period. The seasonality of water table depth (WTD) and flooding stage influences R_s, resulting in seasonal hysteresis in the R_s-soil temperature (T_s) relationship, that is, higher R_s in spring than autumn at mound microsites. This was not the case at low-lying microsites, which had similar hydrologic conditions during both seasons.

[60] The spatial variability and interacting effects of T_s and WTD were accurately described with a nested Q_{10} model where both basal respiration (R_b) and temperature sensitivity (Q_{10}) varied with WTD. The dynamic parameters also reflected the dynamic trends of spatial difference in temperature sensitivity of R_s along with the WTD, which may be associated with the relative contribution of respiratory components. The diel range of R_s was much higher and not attributable to the changes in T_s and WTD, which both had small diel variations. The model fitted to daily R_s had significantly reduced residuals and unexplained variability, indicating that the variability at seasonal timescale was dominated by these two factors, whereas the diel patterns were likely associated with plant activity.

[61] The large amount of CO_2 efflux in a dry year found in this study indicates the potential for large carbon loss from wetland soils under drier climatic conditions. Long-term monitoring is essential to capture the large temporal and spatial variability and better quantification of wetland carbon fluxes. Ecosystem models must consider the dynamics of wetland hydrology to accurately account for wetland carbon balance under climate change.

References

Alm, J., A. Talanov, S. Saarnio, J. Silvola, E. Ikkonen, H. Aaltonen, H. Nykänen, and P. J. Martikainen (1997), Reconstruction of the carbon balance for

microsites in a boreal oligotrophic pine fen, Finland, *Oecologia*, *110*(3), 423–431.

Alm, J., L. Schulman, J. Walden, H. Nykanen, P. J. Martikainen, and J. Silvola (1999), Carbon balance of a boreal bog during a year with an exceptionally dry summer, *Ecology*, *80*(1), 161–174.

Anderson, D. R., K. P. Burnham, and W. L. Thompson (2000), Null hypothesis testing: Problems, prevalence and an alternative, *J. Wildl. Manage.*, *64*, 912–923.

Bahn, M., I. A. Janssens, M. Reichstein, P. Smith, and S. E. Trumbore (2010), Soil respiration across scales: Towards an integration of patterns and processes, *New Phytol.*, *186*(2), 292–296.

Baldocchi, D., E. Falge, and K. Wilson (2001), A spectral analysis of biosphere-atmosphere trace gas flux densities and meteorological variables across hour to multi-year time scales, *Agric. For. Meteorol.*, *107*(1), 1–27.

Barry, W. J., A. S. Garlo, and C. A. Wood (1996), Duplicating the mound-and-pool microtopography of forested wetlands, *Ecol. Restor.*, *14*(1), 15–21.

Blodau, C., N. Basiliko, and T. R. Moore (2004), Carbon turnover in peatland mesocosms exposed to different water table levels, *Biogeosciences*, *67*(3), 331–351.

Bond-Lamberty, B., and A. Thomson (2010), A global database of soil respiration data, *Biogeosciences*, *7*, 1915–1926.

Bond-Lamberty, B., D. Bronson, E. Bladyka, and S. T. Gower (2011), A comparison of trenched plot techniques for partitioning soil respiration, *Soil Biol. Biochem.*, *43*(10), 2108–2114.

Boone, R. D., K. J. Nadelhoffer, J. D. Canary, and J. P. Kaye (1998), Roots exert a strong influence on the temperature sensitivity of soil respiration, *Nature*, *396*(6711), 570–572.

Bridgham, S. D., and C. J. Richardson (1992), Mechanisms controlling soil respiration (CO_2 and CH_4) in southern peatlands, *Soil Biol. Biochem.*, *24*(11), 1089–1099.

Cable, J. M., G. A. Barron-Gafford, K. Ogle, M. Pavao-Zuckerman, R. L. Scott, D. G. Williams, and T. E. Huxman (2012), Shrub encroachment alters sensitivity of soil respiration to temperature and moisture, *J. Geophys. Res.*, *117*, G01001, doi:10.1029/2011JG001757.

Carbone, M. S., and R. Vargas (2008), Automated soil respiration measurements: New information, opportunities and challenges, *New Phytol.*, *177*, 295–297.

Casper, P., S. C. Maberly, G. H. Hall, and B. J. Finlay (2000), Fluxes of methane and carbon dioxide from a small productive lake to the atmosphere, *Biogeosciences*, *49*, 1–19.

Chimner, R. A. (2004), Soil respiration rates of tropical peatlands in Micronesia and Hawaii, *Wetlands*, *24*(1), 51–56.

Davidson, E. A. (2010), Permafrost and wetland carbon stocks, *Science*, *330*(6008), 1176–1177.

Davidson, E. A., and I. A. Janssens (2006), Temperature sensitivity of soil carbon decomposition and feedbacks to climate change, *Nature*, *440*(7081), 165–173.

Davidson, E. A., E. Belk, and R. D. Boone (1998), Soil water content and temperature as independent or confounded factors controlling soil respiration in a temperate mixed hardwood forest, *Global Change Biol.*, *4*(2), 217–227.

Davidson, E. A., I. A. Janssens, and Y. Luo (2006), On the variability of respiration in terrestrial ecosystems: Moving beyond Q_{10}, *Global Change Biol.*, *12*(2), 154–164.

Davidson, E. A., S. Samanta, S. S. Caramori, and K. Savage (2012), The Dual Arrhenius and Michaelis-Menten kinetics model for decomposition of soil organic matter at hourly to seasonal time scales, *Global Change Biol.*, *18*(1), 371–384.

Dinsmore, K. J., U. M. Skiba, M. F. Billett, and R. M. Rees (2009), Effect of water table on greenhouse gas emissions from peatland mesocosms, *Plant Soil*, *318*(1–2), 229–242.

Drewitt, G. B., T. A. Black, Z. Nesic, E. R. Humphreys, E. M. Jork, R. Swanson, G. J. Ethier, T. Griffis, and K. Morgenstern (2002), Measuring forest floor CO_2 fluxes in a Douglas-fir forest, *Agric. For. Meteorol.*, *110*, 299–317.

Ehrenfeld, J. (1995), Microsite differences in surface substrate characteristics in *Chamaecyparis* swamps of the New Jersey Pinelands, *Wetlands*, *15*(2), 183–189.

Falloon, P., C. D. Jones, M. Ades, and K. Paul (2011), Direct soil moisture controls of future global soil carbon changes: An important source of uncertainty, *Global Biogeochem. Cycles*, *25*, GB3010, doi:10.1029/2010GB003938.

Freeman, C., N. Ostle, and H. Kang (2001), An enzymic 'latch' on a global carbon store, *Nature*, *409*, 149.

Freeman, C., N. J. Ostle, N. Fenner, and H. Kang (2004), A regulatory role for phenol oxidase during decomposition in peatlands, *Soil Biol. Biochem.*, *36*, 1663–1667.

Frei, S., K. H. Knorr, S. Peiffer, and J. H. Fleckenstein (2012), Surface microtopography causes hot spots of biogeochemical activity in wetland systems:

A virtual modeling experiment, *J. Geophys. Res.*, *117*, G00N12, doi:10.1029/2012JG002012.

Gaumont-Guay, D., T. A. Black, T. J. Griffis, A. G. Barr, R. S. Jassal, and Z. Nesic (2006), Interpreting the dependence of soil respiration on soil temperature and water content in a boreal aspen stand, *Agric. For. Meteorol.*, *140*(1–4), 220–235.

Goulden, M. L., et al. (1998), Sensitivity of boreal forest carbon balance to soil thaw, *Science*, *279*(5348), 214–217.

Gower, S. T. (2003), Patterns and mechanisms of the forest carbon cycle, *Annu. Rev. Environ. Resour.*, *28*, 169–204.

Högberg, P. (2010), Is tree root respiration more sensitive than heterotrophic respiration to changes in soil temperature?, *New Phytol.*, *188*, 9–10.

Högberg, P., and D. J. Read (2006), Towards a more plant physiological perspective on soil ecology, *Trends Ecol. Evol.*, *21*(10), 548–554.

Ise, T., A. L. Dunn, S. C. Wofsy, and P. R. Moorcroft (2008), High sensitivity of peat decomposition to climate change through water-table feedback, *Nat. Geosci.*, *1*, 763–766.

Jaatinen, K., H. Fritze, J. Laine, and R. Laiho (2007), Effects of short- and long-term water-level drawdown on the populations and activity of aerobic decomposers in a boreal peatland, *Global Change Biol.*, *13*, 491–510.

Janssens, I. A., and K. Pilegaard (2003), Large seasonal changes in Q_{10} of soil respiration in a beech forest, *Global Change Biol.*, *9*(6), 911–918.

Jauhiainen, J., H. Takahashi, J. E. P. Heikkinen, P. J. Martikainen, and H. Vasander (2005), Carbon fluxes from a tropical peat swamp forest floor, *Global Change Biol.*, *11*, 1788–1797.

Johnson, K. A., and R. S. Goody (2011), The Original Michaelis constant: Translation of the 1913 Michaelis–Menten paper, *Biochemistry*, *50*(39), 8264–8269.

Jones, R. H., B. G. Lockaby, and G. L. Somers (1996), Effects of microtopography and disturbance on fine-root dynamics in wetland forests of low-order stream floodplains, *Am. Midl. Nat.*, *136*(1), 57–71.

Jones, R. H., K. O. Henson, and G. L. Somers (2000), Spatial, seasonal, and annual variation of fine root mass in a forested wetland, *J. Torrey Bot. Soc.*, *127*(2), 107–114.

Kim, J., and S. B. Verma (1992), Soil surface CO_2 flux in a Minnesota peatland, *Biogeosciences*, *18*, 37–51.

Kirschbaum, M. U. F. (2006), The temperature dependence of organic-matter decomposition-still a topic of debate, *Soil Biol. Biochem.*, *38*, 2510–2518.

Kuzyakov, Y., and O. Gavrichkova (2010), REVIEW: Time lag between photosynthesis and carbon dioxide efflux from soil: A review of mechanisms and controls, *Global Change Biol.*, *16*(12), 3386–3406.

Kvalseth, T. O. (1985), Cautionary note about R^2, *Am. Stat.*, *39*(4), 279–285.

Laiho, R. (2006), Decomposition in peatlands: Reconciling seemingly contrasting results on the impacts of lowered water levels, *Soil Biol. Biochem.*, *38*(8), 2011–2024.

Larcher, W. (2003), *Physiological Plant Ecology: Ecophysiology and Stress Physiology of Functional Groups*, Springer-Verlag, Berlin, Germany.

Lavigne, M. B., R. Boutin, R. J. Foster, G. Goodine, P. Y. Bernier, and G. Robitaille (2003), Soil respiration responses to temperature are controlled more by roots than by decomposition in balsam fir ecosystems, *Can. J. For. Res.*, *33*(9), 1744–1753.

Law, B. E., F. M. Kelliher, D. D. Baldocchi, P. M. Anthoni, J. Irvine, D. Moore, and S. Van Tuyl (2001), Spatial and temporal variation in respiration in a young ponderosa pine forest during a summer drought, *Agric. For. Meteorol.*, *110*(1), 27–43.

Lee, X., H.-J. Wu, J. Sigler, C. Oishi, and T. Siccama (2004), Rapid and transient response of soil respiration to rain, *Global Change Biol.*, *10*(6), 1017–1026.

Lellei-Kovács, E., E. Kovács-Láng, Z. Botta-Dukát, T. Kalapos, B. Emmett, and C. Beier (2011), Thresholds and interactive effects of soil moisture on the temperature response of soil respiration, *Eur. J. Soil Biol.*, *47*, 247–255.

Liu, Q., N. T. Edwards, W. M. Post, L. Gu, J. Ledford, and S. Lenhart (2006), Temperature-independent diel variation in soil respiration observed from a temperate deciduous forest, *Global Change Biol.*, *12*(11), 2136–2145.

Lloyd, J., and J. A. Taylor (1994), On the temperature dependence of soil respiration, *Funct. Ecol.*, *8*(3), 315–323.

Lugo, A. E., S. Brown, and M. Brinson (1990), *Forested Wetlands*, Elsevier, Amsterdam, Netherlands.

Luken, J. O., and W. D. Billings (1985), The influence of microtopographic heterogeneity on carbon dioxide efflux from a subarctic bog, *Holarctic Ecol.*, *8*, 306–312.

Luo, Y., and X. Zhou (2006), *Soil Respiration and the Environment*, 316 pp., Elsevier/Academic Press, Amsterdam.

Maberly, S. C. (1996), Diel, episodic and seasonal changes in pH and concentrations of inorganic carbon in a productive lake, *Freshwater Biol.*, *35*, 579–598.

Mahecha, M. D., et al. (2010), Global convergence in the temperature sensitivity of respiration at ecosystem level, *Science*, *329*(5993), 838–840.

Mäkiranta, P., R. Laiho, H. Fritze, J. Hytönen, J. Laine, and K. Minkkinen (2009), Indirect regulation of heterotrophic peat soil respiration by water level via microbial community structure and temperature sensitivity, *Soil Biol. Biochem.*, *41*(4), 695–703.

Mast, M. A., K. P. Wickland, R. T. Striegl, and D. W. Clow (1998), Winter fluxes of CO_2 and CH_4 from subalpine soils in Rocky Mountain National Park, Colorado, *Global Biogeochem. Cycles*, *12*(4), 607–620.

Mitsch, W. J., and J. G. Gosselink (2007), *Wetlands*, John Wiley Inc., New York, N. Y., USA.

Moore, T. R. (1986), Carbon dioxide evolution from subarctic peatlands in eastern Canada, *Arct. Alp. Res.*, *18*(2), 189–193.

Moore, T. R., and M. Dalva (1993), The influence of temperature and water table position on carbon dioxide and methane emissions from laboratory columns of peatland soils, *J. Soil Sci.*, *44*, 651–664.

Moorhead, K. K., and M. M. Brinson (1995), Response of wetlands to rising sea level in the lower coastal plain of North Carolina, *Ecol. Appl.*, *5*(1), 261–271.

Morén, A.-S., and A. Lindroth (2000), CO_2 exchange at the floor of a boreal forest, *Agric. For. Meteorol.*, *101*, 1–14.

Motulsky, H., and A. Christopoulos (2004), *Fitting Models to Biological Data Using Linear and Nonlinear Regression: A Practical Guide to Curve Fitting*, Oxford University Press, New York, N. Y., USA.

Noormets, A., et al. (2008), Moisture sensitivity of ecosystem respiration: Comparison of 14 forest ecosystems in the Upper Great Lakes Region, USA, *Agric. For. Meteorol.*, *148*, 216–230.

Phillips, S. C., R. K. Varner, S. Frolking, J. W. Munger, J. L. Bubier, S. C. Wofsy, and P. M. Crill (2010), Interannual, seasonal, and diel variation in soil respiration relative to ecosystem respiration at a wetland to upland slope at Harvard Forest, *J. Geophys. Res.*, *115*, G02019, doi:10.1029/2008JG000858.

Reichstein, M., J. D. Tenhunen, O. Roupsard, J.-M. Ourcival, S. Rambal, S. Dore, and R. Valentini (2002), Ecosystem respiration in two Mediterranean evergreen Holm Oak forests: Drought effects and decomposition dynamics, *Funct. Ecol.*, *16*, 27–39.

Reichstein, M., J.-A. Subke, A. C. Angeli, and J. D. Tenhunen (2005), Does the temperature sensitivity of decomposition of soil organic matter depend upon water content, soil horizon, or incubation time?, *Global Change Biol.*, *11*(10), 1754–1767.

Riveros-Iregui, D. A., R. E. Emanuel, D. J. Muth, B. L. McGlynn, H. E. Epstein, D. L. Welsch, V. J. Pacific, and J. M. Wraith (2007), Diurnal hysteresis between soil CO_2 and soil temperature is controlled by soil water content, *Geophys. Res. Lett.*, *34*, L17404, doi:10.1029/2007GL030938.

Ruehr, N., A. Knohl, and N. Buchmann (2010), Environmental variables controlling soil respiration on diurnal, seasonal and annual time-scales in a mixed mountain forest in Switzerland, *Biogeosciences*, *98*(1), 153–170.

Sampson, D. A., I. A. Janssens, J. Curiel Yuste, and R. Ceulemans (2007), Basal rates of soil respiration are correlated with photosynthesis in a mixed temperate forest, *Global Change Biol.*, *13*(9), 2008–2017.

Savage, K. E., and E. A. Davidson (2001), Interannual variation of soil respiration in two New England forests, *Global Biogeochem. Cycles*, *15*(2), 337–350.

Savage, K. E., and E. A. Davidson (2003), A comparison of manual and automated systems for soil CO_2 flux measurements: Trade-offs between spatial and temporal resolution, *J. Exp. Bot.*, *54*(384), 891–899.

Schreader, C. P., W. R. Rouse, T. J. Griffis, L. D. Boudreau, and P. D. Blanken (1998), Carbon dioxide fluxes in a northern fen during a hot, dry summer, *Global Biogeochem. Cycles*, *12*(4), 729–740.

Seber, G. A. F., and C. J. Wild (2003), *Nonlinear Regression*, Wiley-Interscience, Hoboken, N. J., USA.

Silvola, J., J. Alm, U. Ahlholm, H. Nykanen, and P. J. Martikainen (1996), CO_2 fluxes from peat in boreal mires under varying temperature and moisture conditions, *J. Ecol.*, *84*, 219–228.

Smith, C. J., R. D. Delaune, and J. W. H. Patrick (1983), Carbon dioxide emission and carbon accumulation in coastal wetlands, *Estuarine Coastal Shelf Sci.*, *17*, 21–29.

Subke, J.-A., and M. Bahn (2010), On the 'temperature sensitivity' of soil respiration: Can we use the immeasurable to predict the unknown?, *Soil Biol. Biochem.*, *42*, 1653–1656.

Sullivan, P., S. T. Arens, R. Chimner, and J. Welker (2008), Temperature and microtopography interact to control carbon cycling in a high Arctic fen, *Ecosystems*, *11*(1), 61–76.

Sun, G., S. G. McNulty, D. M. Amatya, R. W. Skaggs, L. W. Swift Jr., J. P. Shepard, and H. Riekerk (2002), A comparison of the watershed hydrology of coastal forested wetlands and the mountainous uplands in the Southern US, *J. Hydrol.*, *263*(1–4), 92–104.

Tang, J. W., D. D. Baldocchi, and L. Xu (2005a), Tree photosynthesis modulates soil respiration on a diurnal time scale, *Global Change Biol.*, *11*(8), 1298–1304.

Tang, J. W., L. Misson, A. Gershenson, W. X. Cheng, and A. H. Goldstein (2005b), Continuous measurements of soil respiration with and without

roots in a ponderosa pine plantation in the Sierra Nevada Mountains, *Agric. For. Meteorol.*, *132*(3–4), 212–227.

Thomas, K. L., J. Benstead, K. L. Davies, and D. Lloyd (1996), Role of wetland plants in the diurnal control of CH_4 and CO_2 fluxes in peat, *Soil Biol. Biochem.*, *28*(1), 17–23.

Trettin, C. C., and M. F. Jurgensen (2003), Carbon cycling in wetland forest soils, in *The Potential of U.S. Forest Soils to Sequester Carbon and Mitigate the Greenhouse Effect*, edited by J. M. Kimble et al., pp. 311–331, CRC Press, Boca Raton.

Van der Ploeg, M. J., W. M. Appels, D. G. Cirkel, M. R. Oosterwoud, J.-P. M. Witte, and S. E. A. T. M. van der Zee (2012), Microtopography as a driving mechanism for ecohydrological processes in shallow groundwater systems, *Vadose Zone J.*, *11*(3), doi:10.2136/vzj2011.0098.

Vargas, R., and M. F. Allen (2008), Environmental controls and the influence of vegetation type, fine roots and rhizomorphs on diel and seasonal variation in soil respiration, *New Phytol.*, *179*(2), 460–471.

Vicca, S., I. A. Janssens, H. Flessa, S. Fiedler, and H. F. Jungkunst (2009), Temperature dependence of greenhouse gas emissions from three hydromorphic soils at different groundwater levels, *Geobiology*, *7*(4), 465–476.

Vincent, G., A. R. Shahriari, E. Lucot, P.-M. Badot, and D. Epron (2006), Spatial and seasonal variations in soil respiration in a temperate deciduous forest with fluctuating water table, *Soil Biol. Biochem.*, *38*, 2527–2535.

Waddington, J. M., and N. T. Roulet (1996), Atmosphere-wetland carbon exchanges: Scale dependency of CO_2 and CH_4 exchange on the developmental topography of a peatland, *Global Biogeochem. Cycles*, *10*(2), 233–245.

Wen, X. F., H. M. Wang, J. L. Wang, G. R. Yu, and X. M. Sun (2010), Ecosystem carbon exchanges of a subtropical evergreen coniferous plantation subjected to seasonal drought, 2003–2007, *Biogeosciences*, *7*(1), 357–369.

Wheeler, B. D. (1999), Water and plants in freshwater wetlands, in *Eco-Hydrology: Plants and Water in Terrestrial and Aquatic Environments*, edited by A. J. Baird and R. L. Wilby, pp. 127–180, Wilby, Routledge, London, U. K.

Yuan, W., et al. (2011), Redefinition and global estimation of basal ecosystem respiration rate, *Global Biogeochem. Cycles*, *25*, GB4002, doi:10.1029/2011GB004150.

Zhou, X., Y. Luo, C. Gao, P. S. J. Verburg, J. A. I. Arnone, A. Darrouzet-Nardi, and D. S. Schimel (2010), Concurrent and lagged impacts of an anomalously warm year on autotrophic and heterotrophic components of soil respiration: A deconcolution analysis, *New Phytol.*, *187*, 184–198.